PROCEEDINGS OF SCIENCE

Antistatic-antistatic-light-light potentials from lattice QCD

Lasse Mueller,[a,*] **Pedro Bicudo,**[b] **Marina Krstic Marinkovic**[c] **and Marc Wagner**[a,d]

[a] *Goethe-Universität Frankfurt am Main, Institut für Theoretische Physik, Max-von-Laue-Straße 1, D-60438 Frankfurt am Main, Germany*

[b] *CeFEMA, Dep. Física, Instituto Superior Técnico, Universidade de Lisboa, Av. Rovisco Pais, 1049-001 Lisboa, Portugal*

[c] *Institut für Theoretische Physik, Wolfgang-Pauli-Straße 27, ETH Zürich, 8093 Zürich, Switzerland*

[d] *Helmholtz Research Academy Hesse for FAIR, Campus Riedberg, Max-von-Laue-Straße 12, D-60438 Frankfurt am Main, Germany*

E-mail: lmueller@itp.uni-frankfurt.de, bicudo@tecnico.ulisboa.pt, marinama@ethz.ch, mwagner@itp.uni-frankfurt.de

We present results for tetraquark potentials of two static anti-quarks $\bar{b}\bar{b}$ in the presence of two light quarks u and/or d. We improve on existing results by computing the static potential also for off-axis separations, which increases the number of data points significantly. Moreover, we compute for the first time $\bar{b}\bar{b}us$ potentials.

The 40th International Symposium on Lattice Field Theory (Lattice 2023)
July 31st - August 4th, 2023
Fermi National Accelerator Laboratory

*Speaker

© Copyright owned by the author(s) under the terms of the Creative Commons Attribution-NonCommercial-NoDerivatives 4.0 International License (CC BY-NC-ND 4.0).

PoS(LATTICE2023)064

1. Introduction

With the recent discovery of the T_{cc} tetraquark at LHCb [1, 2] studies of four-quark systems with two heavy anti-quarks and two light quarks have become particularly important. There have been several lattice computations in the past years studying such systems with Lüscher's finite volume method [3–10] and the HAL-QCD method [11]. In this work we use a different approach by computing potentials between two static anti-quarks in the presence of two light quarks (for previous related work see e.g. Refs. [12, 13]). Such potentials provide insights concerning the possible formation of tetraquarks and allow to study their existence and properties in the Born-Oppenheimer-approximation. For now, such potentials have only been used to study $\bar{b}\bar{b}qq$ tetraquarks [14–19], but they could also be used to investigate $\bar{b}\bar{c}qq$. In the future one might even consider investigating the T_{cc} tetraquark, which would, however, require additional computations of relativistic corrections (see e.g. Refs. [20, 21], where such corrections are discussed for the ordinary static potential).

In this work we significantly improve on existing results [13] for the $\bar{b}\bar{b}ud$ system and we present for the first time results for the $\bar{b}\bar{b}us$ system.

2. Creation operators and correlation functions

We use creation operators with two anti-b quarks and two light u/d quarks,

$$O^{I,\Gamma}_{BB}(\mathbf{r}_1,\mathbf{r}_2) = (C\Gamma)_{AB}\left(C\tilde{\Gamma}\right)_{CD}\left(\bar{b}^a_C(\mathbf{r}_1)u^a_A(\mathbf{r}_1)\;\bar{b}^b_D(\mathbf{r}_2)d^b_B(\mathbf{r}_2) \mp (u\leftrightarrow d)\right), \tag{1}$$

where $\mp$ corresponds to isospin $I=0$ and $I=1$, respectively, $C=\gamma_0\gamma_2$ is the charge conjugation matrix and A,B,C,D denote spin and a,b color indices. In the static limit the spins of the $\bar{b}$ quarks are irrelevant and the four choices $\tilde{\Gamma}\in\{(1+\gamma_0)\gamma_5, (1+\gamma_0)\gamma_j\}$ lead to the same correlation function. Γ couples the spin components of the light quarks and, thus, determines the quantum numbers Λ^ϵ_η as discussed in the next section.

Temporal correlation functions of these creation operators can be expressed in terms of propagators,

$$\begin{aligned}
C^{I,\Gamma}_{BB}(\mathbf{r}_2-\mathbf{r}_1,t_2-t_1) &= \langle\Omega|O^{I,\Gamma\,\dagger}_{BB}(\mathbf{r}_1,\mathbf{r}_2;t_2)O^{I,\Gamma}_{BB}(\mathbf{r}_1,\mathbf{r}_2;t_1)|\Omega\rangle \propto \\
&\propto \Bigg\langle \left(\gamma_0\Gamma^\dagger\gamma_0\right)_{BA}\Gamma_{CD}\Bigg(\\
&\mathrm{Tr}_c\left[U(\mathbf{r}_1,t_2;\mathbf{r}_1,t_1)\left(M_q^{-1}\right)_{CA}(\mathbf{r}_1,t_1;\mathbf{r}_1,t_2)\right]\times\mathrm{Tr}_c\left[U(\mathbf{r}_2,t_2;\mathbf{r}_2,t_1)\left(M_q^{-1}\right)_{DB}(\mathbf{r}_2,t_1;\mathbf{r}_2,t_2)\right] \\
&\pm\mathrm{Tr}_c\left[U(\mathbf{r}_1,t_2;\mathbf{r}_1,t_1)\left(M_q^{-1}\right)_{CA}(\mathbf{r}_1,t_1;\mathbf{r}_2,t_2)\;U(\mathbf{r}_2,t_2;\mathbf{r}_2,t_1)\left(M_q^{-1}\right)_{DB}(\mathbf{r}_2,t_1;\mathbf{r}_1,t_2)\right]\Bigg)\Bigg\rangle \equiv \\
&\equiv
\end{aligned} \tag{2}$$

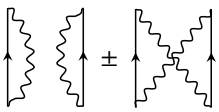

where $t_2-t_1>0$, Tr_c denotes the trace in color space, U is a straight path of gauge links in temporal direction (represented by a straight line in the diagram) and M_q^{-1} a light quark propagator (represented by a wiggly line).

PoS(LATTICE2023)064

	$I=0$		$I=1$	
Γ	Λ_η^ϵ	shape	Λ_η^ϵ	shape
$\gamma_5+\gamma_0\gamma_5$	Σ_u^+	A,SS	Σ_g^+	R,SS
1	Σ_g^-	A,SP	Σ_u^-	R,SP
γ_0	Σ_u^-	R,SP	Σ_g^-	A,SP
$\gamma_5-\gamma_0\gamma_5$	Σ_u^+	A,PP	Σ_g^+	R,PP
$\gamma_3+\gamma_0\gamma_3$	Σ_g^-	R,SS	Σ_u^-	A,SS
$\gamma_3\gamma_5$	Σ_g^+	A,SP	Σ_u^+	R,SP
$\gamma_0\gamma_3\gamma_5$	Σ_u^+	R,SP	Σ_g^+	A,SP
$\gamma_3-\gamma_0\gamma_3$	Σ_g^-	R,PP	Σ_u^-	A,PP
$\gamma_{1/2}+\gamma_0\gamma_{1/2}$	Π_g	R,SS	Π_u	A,SS
$\gamma_{1/2}\gamma_5$	Π_g	A,SP	Π_u	R,SP
$\gamma_0\gamma_{1/2}\gamma_5$	Π_u	R,SP	Π_g	A,SP
$\gamma_{1/2}-\gamma_0\gamma_{1/2}$	Π_g	R,PP	Π_u	A,PP

Table 1: Quantum numbers and properties of the resulting $\bar{b}\bar{b}ud$ potentials: A = attractive, R = repulsive; SS, SP ,PP = asymptotic value $2m_B$, $m_B+m_{B_0^*}$, $2m_{B_0^*}$.

We normalize these correlation functions by dividing by the square of the correlation function for a single B meson. The large-t behavior is then given by

$$\frac{C_{BB}^{I,\Gamma}(\mathbf{r},t)}{(C_B(t))^2} \xrightarrow[t\to\infty]{} A\exp\left(-\left(V_{BB}^{I,\Lambda_\eta^\epsilon}(\mathbf{r})-2m_B\right)t\right), \tag{3}$$

i.e. the zero point of the energy corresponds to two times the B meson mass.

3. Quantum numbers of anti-static-anti-static potentials

In addition to isospin I, our $\bar{b}\bar{b}ud$ potentials can be characterized by the following quantum numbers:

- $\Lambda=\Sigma,\Pi$: Total angular momentum with respect to the separation axis of the anti-quarks.
- $\eta=+,-\equiv g,u$: Behavior under parity.
- $\epsilon=+,-$: Behavior under reflection along an axis perpendicular to the separation axis.

In Table 1 we relate all possible independent choices for Γ with their corresponding Λ_η^ϵ quantum numbers.

4. Lattice setup

For our computations we resort to 100 gauge link configurations from a single ensemble generated within the CLS effort [23, 24] using two dynamical flavours of $O(a)$-improved Wilson-quarks and the Wilson plaquette action. The lattice size is $(L/a)^3\times T/a = 32^3\times 64$ with lattice

PoS(LATTICE2023)064

spacing $a \approx 0.0755\,\text{fm}$ and pion mass $m_\pi \approx 331\,\text{MeV}$. The static action of the $\bar{b}$ quarks is the HYP2 static action.

We use stochastic timeslice propagators for the light quarks with 12 stochastic sources per timeslice on 8 timeslices per gauge link configuration.

We crudely optimize the ground state overlaps generated by our creation operators (1) by using Gaussian smearing for the quark fields with APE smeared spatial links. We performed $N_{\text{Gauss}} = 50$ steps of Gaussian smearing with $\kappa = 0.5$ and $N_{\text{APE}} = 30$ steps of APE-smearing with $\alpha_{\text{APE}} = 30$ (With the smearing algorithms and notation consistent with [25]).

Our computations were done using the openQ*D codebase [26].

5. Results for $\bar{b}\bar{b}ud$ potentials

We extract $\bar{b}\bar{b}ud$ potentials from the large-t behavior of correlation functions (3). We consider separations $\mathbf{r}$ along the coordinate axes up to $|\mathbf{r}| = 16a$. To obtain a fine spatial resolution in the interesting region of small separations, we also consider off-axis separations. We compute all possible off-axis separations for $|\mathbf{r}| \leq 4a$ and a subset of off-axis separations, containing the space diagonal (x, x, x), the plane diagonal $(x, x, 0)$ and all separations of the form $(x, 1, 2)$ for $|\mathbf{r}| \leq 10a$ (with $x \in \mathbb{Z}$ and averaging over all permutations). This yields about twenty-five additional data points. To reduce lattice artifacts, in particular at small $|\mathbf{r}|$, we employ tree level improvement [27]. In Fig. 1 we show the corresponding results for the 24 independent creation operators collected in Table 1. Each potential is either attractive or repulsive and has one of three characteristic asymptotic values $2m_B$, $m_B + m_{B_0^*}$ and $2m_{B_0^*}$ (m_B denotes the mass of the negative parity B or B^* meson, which are degenerate in the static limit; $m_{B_0^*}$ denotes the mass of the positive parity B_0^* or B_1^* meson, which are degenerate in the static limit and are around 400 MeV heavier than the B or B^* meson; see e.g. Ref. [25]). Our results are in qualitative agreement with existing results obtained around a decade ago restricted to on-axis separations [13].

Note that we do not consider correlation matrices, but only correlation functions with the same creation operator at both times t_1 and t_2. The consequence is that excited potentials in a given Λ_η^ϵ sector (e.g. the orange and green curves in the upper left plot of Fig. 1) might be contaminated by lower potentials (the blue and orange curves in the same plot).

From a phenomenological point of view attractive potentials with asymptotic value $2m_B$ are of particular interest, since they are the best candidates to host bound states or resonances, which correspond to $\bar{b}\bar{b}ud$ tetraquarks. The most attractive potential has $I = 0$ and $\Lambda_\eta^\epsilon = \Sigma_u^+$, while there are two related less attractive potentials with $I = 1$ and $\Lambda_\eta^\epsilon = \Sigma_u^-, \Pi_u$. All three potentials can be parameterized consistently using an ansatz for a screened $1/r$ potential,

$$V(r) = -\frac{\alpha_1}{r} \exp\left(-\left(\frac{r}{d}\right)^p\right). \tag{4}$$

We show these potentials with corresponding fits (blue curves) in Fig. 2. For comparison, we also show the result from Ref. [13] for the $I = 0$ and Σ_u^+ potential obtained at similar pion mass (red curve), which is consistent with our results from this work. The $I = 1$ and Σ_u^- and Π_u potentials at intermediate separations $0.4\,\text{fm} \lesssim r \lesssim 0.7\,\text{fm}$ seem to be slightly above the asymptotic value $2m_B$. Thus, there might be a weak repulsion caused by one-pion exchange. We plan to investigate this in more detail in the future by carrying out computations at smaller pion masses.

PoS(LATTICE2023)064

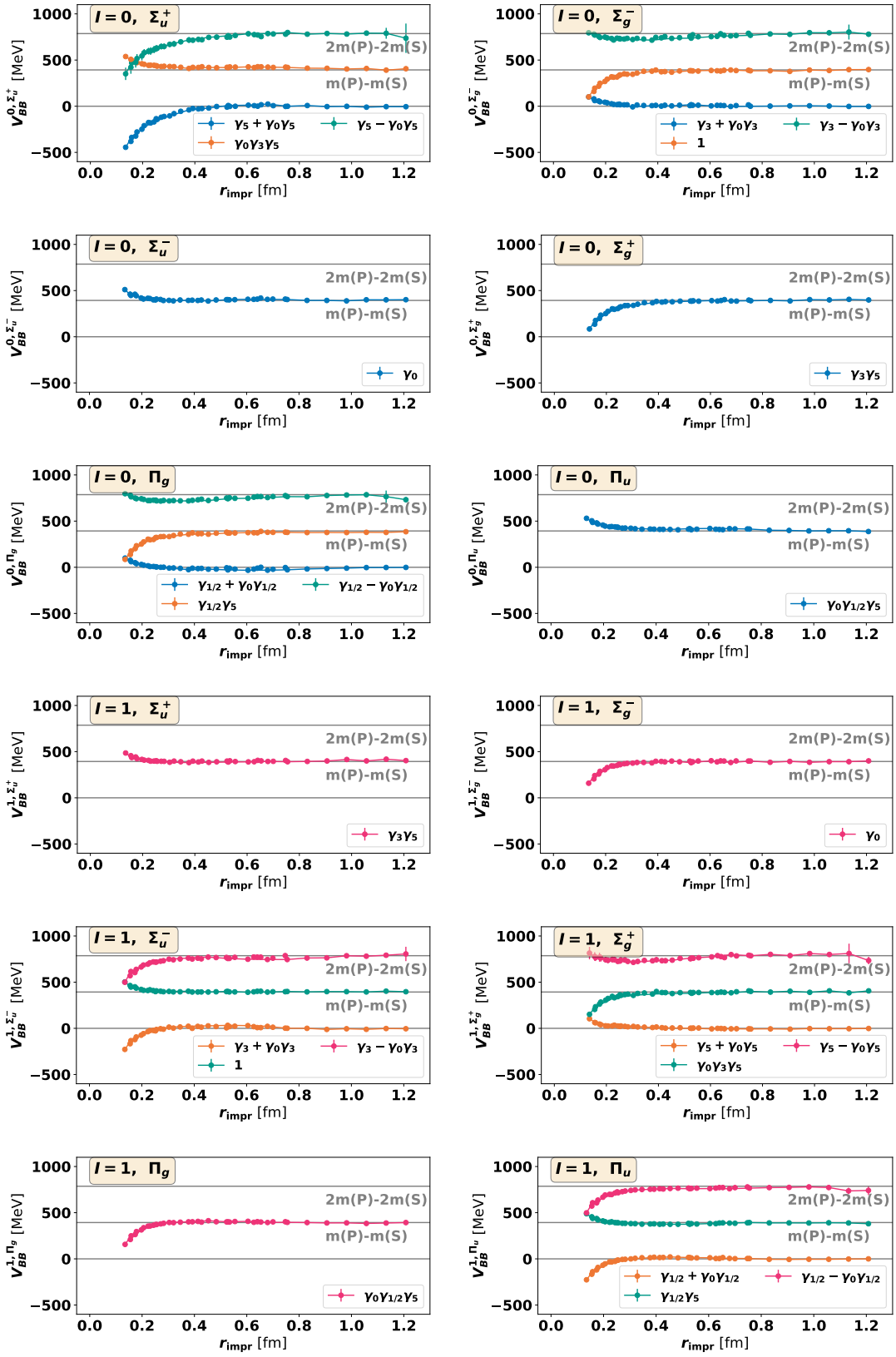

Figure 1: $\bar{b}\bar{b}ud$ potentials extracted from correlation functions corresponding to the 24 independent creation operators collected in Table 1.

PoS(LATTICE2023)064

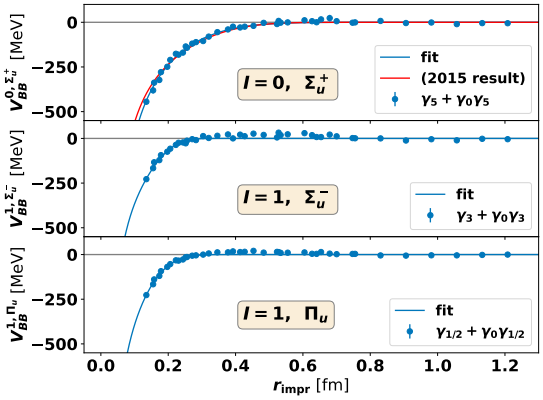

Figure 2: Attractive $\bar{b}\bar{b}ud$ potentials with asymptotic value $2m_B$ (blue curves represent fits with the ansatz (4); the red curve is a result from Ref. [13]).

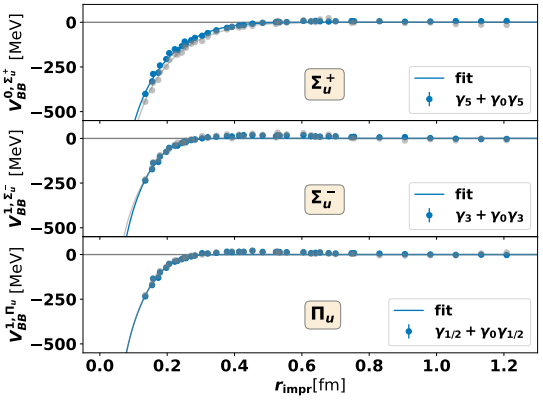

Figure 3: Attractive $\bar{b}\bar{b}us$ potentials with asymptotic value $m_B + m_{B_s}$ (blue curves represent fits with the ansatz (4)). The gray potentials represent the $\bar{b}\bar{b}ud$ results.

6. Results for $\bar{b}\bar{b}us$ potentials

In this work we compute for the first time also $\bar{b}\bar{b}us$ potentials. In contrast to the $\bar{b}\bar{b}ud$ case, the two light quark propagators are different and, thus, the correlation functions contain four diagrams,

$$C^{\Gamma}_{BB_s}(\mathbf{r}_2 - \mathbf{r}_1, t_2 - t_1) \equiv$$ 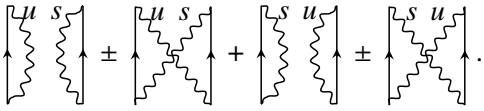 (5)

Due to the mass difference of the u and the s quark, there is only an approximate light flavor symmetry and the $I = 0$ and $I = 1$ sectors from the $\bar{b}\bar{b}ud$ case are not anymore separated for $\bar{b}\bar{b}us$. However, the three attractive potentials with asymptotic value $m_B + m_{B_s}$ can still be extracted from their corresponding correlation functions without additional difficulties, because excited potentials with the same quantum numbers Λ_η^ϵ are around 400 MeV above. We show these $\bar{b}\bar{b}us$ potentials in Fig. 3. As expected, they are similar to their $\bar{b}\bar{b}ud$ counterparts, yet slightly less binding.

Acknowledgements

We acknowledge useful discussions with Marco Catillo, Mika Lauk, Daniel Mohler and Carolin Schlosser.

L.M. acknowledges support by a Karin and Carlo Giersch Scholarship of the Giersch foundation. M.W. and L.M. acknowledge support by the Deutsche Forschungsgemeinschaft (DFG, German Research Foundation) – project number 457742095. M.W. acknowledges support by the Heisenberg Programme of the Deutsche Forschungsgemeinschaft (DFG, German Research Foundation) – project number 399217702. PB thanks the support of CeFEMA funded by FCT under contract UIDB/04540/2020. This work was performed in part at Aspen Center for Physics, which is supported by National Science Foundation grant PHY-2210452; the research was additionally

PoS(LATTICE2023)064

supported in part by the National Science Foundation Grant No. NSF PHY-1748958. We acknowledge access to Piz Daint at the Swiss National Supercomputing Centre, Switzerland under the ETHZ's share with the project ID eth8. Calculations were conducted on the GOETHE-HLR and on the FUCHS-CSC high-performance computers of the Frankfurt University. We would like to thank HPC-Hessen, funded by the State Ministry of Higher Education, Research and the Arts, for programming advice.

References

[1] R. Aaij *et al.* [LHCb], Nature Phys. **18**, no.7, 751-754 (2022) [arXiv:2109.01038 [hep-ex]].

[2] R. Aaij *et al.* [LHCb], Nature Commun. **13**, no.1, 3351 (2022) [arXiv:2109.01056 [hep-ex]].

[3] A. Francis, R. J. Hudspith, R. Lewis and K. Maltman, Phys. Rev. Lett. **118**, no.14, 142001 (2017) [arXiv:1607.05214 [hep-lat]].

[4] A. Francis, R. J. Hudspith, R. Lewis and K. Maltman, Phys. Rev. D **99**, no.5, 054505 (2019) [arXiv:1810.10550 [hep-lat]].

[5] P. Junnarkar, N. Mathur and M. Padmanath, Phys. Rev. D **99**, no.3, 034507 (2019) [arXiv:1810.12285 [hep-lat]].

[6] L. Leskovec, S. Meinel, M. Pflaumer and M. Wagner, Phys. Rev. D **100**, no.1, 014503 (2019) [arXiv:1904.04197 [hep-lat]].

[7] R. J. Hudspith, B. Colquhoun, A. Francis, R. Lewis and K. Maltman, Phys. Rev. D **102**, 114506 (2020) doi:10.1103/PhysRevD.102.114506 [arXiv:2006.14294 [hep-lat]].

[8] P. Mohanta and S. Basak, Phys. Rev. D **102**, no.9, 094516 (2020) [arXiv:2008.11146 [hep-lat]].

[9] S. Meinel, M. Pflaumer and M. Wagner, Phys. Rev. D **106**, no.3, 034507 (2022) [arXiv:2205.13982 [hep-lat]].

[10] M. Padmanath, A. Radhakrishnan and N. Mathur, [arXiv:2307.14128 [hep-lat]].

[11] T. Aoki, S. Aoki and T. Inoue, Phys. Rev. D **108**, no.5, 054502 (2023) [arXiv:2306.03565 [hep-lat]].

[12] M. Wagner [ETM], PoS **LATTICE2010**, 162 (2010) [arXiv:1008.1538 [hep-lat]].

[13] P. Bicudo, K. Cichy, A. Peters and M. Wagner, Phys. Rev. D **93**, no.3, 034501 (2016) [arXiv:1510.03441 [hep-lat]].

[14] P. Bicudo and M. Wagner, Phys. Rev. D **87**, no.11, 114511 (2013) [arXiv:1209.6274 [hep-ph]].

[15] Z. S. Brown and K. Orginos, Phys. Rev. D **86**, 114506 (2012) [arXiv:1210.1953 [hep-lat]].

[16] P. Bicudo, K. Cichy, A. Peters, B. Wagenbach and M. Wagner, Phys. Rev. D **92**, no.1, 014507 (2015) [arXiv:1505.00613 [hep-lat]].

PoS(LATTICE2023)064

[17] P. Bicudo, J. Scheunert and M. Wagner, Phys. Rev. D **95**, no.3, 034502 (2017) [arXiv:1612.02758 [hep-lat]].

[18] P. Bicudo, M. Cardoso, A. Peters, M. Pflaumer and M. Wagner, Phys. Rev. D **96**, no.5, 054510 (2017) [arXiv:1704.02383 [hep-lat]].

[19] J. Hoffmann, A. Zimermmane-Santos and M. Wagner, PoS **LATTICE2022**, 262 (2023) [arXiv:2211.15765 [hep-lat]].

[20] A. Pineda and A. Vairo, Phys. Rev. D **63**, 054007 (2001) [erratum: Phys. Rev. D **64**, 039902 (2001)] [arXiv:hep-ph/0009145 [hep-ph]].

[21] M. Eichberg and M. Wagner, [arXiv:2311.06560 [hep-lat]].

[22] K. Jansen *et al.* [ETM], JHEP **12**, 058 (2008) [arXiv:0810.1843 [hep-lat]].

[23] P. Fritzsch, F. Knechtli, B. Leder, M. Marinkovic, S. Schaefer, R. Sommer and F. Virotta, Nucl. Phys. B **865**, 397-429 (2012) [arXiv:1205.5380 [hep-lat]].

[24] G. P. Engel, L. Giusti, S. Lottini and R. Sommer, Phys. Rev. D **91**, no.5, 054505 (2015) [arXiv:1411.6386 [hep-lat]].

[25] K. Jansen *et al.* [ETM], JHEP **12**, 058 (2008) [arXiv:0810.1843 [hep-lat]].

[26] I. Campos *et al.* [RC*], Eur. Phys. J. C **80**, no.3, 195 (2020) [arXiv:1908.11673 [hep-lat]].

[27] R. Sommer, Nucl. Phys. B **411**, 839-854 (1994) [arXiv:hep-lat/9310022 [hep-lat]].

PoS(LATTICE2023)064